arXiv:1402.1487v1 [quant-ph] 6 Feb 2014

Truncated coherent states and photon-addition

S. Sivakumar

Materials Physics Division

Indira Gandhi Centre for Atomic Research

Kalpakkam 603 102 INDIA

Email: siva@igcar.gov.in

February 10, 2014

Abstract

A class of states of the electromagnetic field involving superpositions of all the excited states above a specified low energy eigenstate of the electromagnetic field is introduced. These states and the photon-added coherent states are shown to be the limiting cases of a generalized photon-added coherent states. This new class of states is nonclassical, non-Gaussian and has equal uncertainties in the field quadratures. For suitable choices of parameters, these uncertainties are very close to those of the coherent states. Nevertheless, these states exhibit sub-Poissonian photon number distribution, which is a nonclassical feature. Under suitable approximations, these states become the generalized Bernoulli states of the field. Nonclassicality of these states is quantified using their entanglement potential.

PACS: 42.50. -p, 42.50.Lc, 03.67.Bg

Keywords: Truncated Coherent states, photon-added coherent states, inverse boson operators, entanglement potential

1 Introduction

Quantum theory stipulates a lower bound on the product of the uncertainties of in a pair of non-commuting observables such as the position and momentum, the phase and particle number, etc. In the context of the position-momentum uncertainty relation $\Delta x \Delta p \geq \hbar/2$, there are states which satisfy $\Delta x \Delta p = \hbar/2$. Such states are called minimum uncertainty states(MUS), for example, the coherent states and the squeezed vacuum. Of all the MUS, the coherent states $|\alpha\rangle$[1, 2],

$$|\alpha\rangle = \exp\left(-\frac{|\alpha|^2}{2}\right) \sum_{n=0}^{\infty} \frac{\alpha^n}{\sqrt{n!}} |n\rangle, \tag{1}$$

defined for every complex number α, are very special as their phase space distributions (P- and Wigner-distributions) are well-defined probability densities[3]. For that reason, the coherent states are considered to be "classical" among the quantum states. Any other pure state of a harmonic oscillator is non-classical, in the sense that its phase space distribution (P-function or Wigner) fails to be non-negative. Interestingly, superpositions of two coherent states generate non-classical states; the even and odd coherent states[4, 5, 6] are prime examples of such states. In the case of the electromagnetic field, photon-addition and state truncation are two other processes to create non-classical states from coherent states[7, 8]. Both these routes have been experimentally realized[9, 10, 11, 12]. In the process of state truncation, a finite number of Fock states are retained in the coherent states. Truncated

coherent states (TCS) are defined as[13, 14, 15, 16]

$$|\alpha, N; u\rangle = N_u \sum_{n=0}^{N} \frac{\alpha^n}{\sqrt{n!}} |n\rangle, \tag{2}$$

where N_u^{-2} is $\exp(|\alpha|^2)[1 - \gamma(N+1, |\alpha|^2)/N!]$. The incomplete Gamma function $\gamma(N, x)$ [17]is defined as

$$\gamma(N, x) = (N-1)! \left[1 - \exp(-x) \sum_{j=0}^{N-1} \frac{x^j}{j!}\right], \tag{3}$$

N being the order of the function. Since there is an upper limit on the number of Fock states involved in the superposition, this state is referred as upper-truncated coherent states (UTCS). These experimentally realizable states have been studied extensively for their nonclassical features[14, 18, 19, 20, 21]. In the limit $N \to \infty$, $|\alpha, N; u\rangle$ becomes the coherent state $|\alpha\rangle$. Another class of states associated with the UTCS is defined as follows:

$$|\alpha, N; l\rangle = N_l \sum_{n=0}^{\infty} \frac{\alpha^n}{\sqrt{(N+1+n)!}} |N+1+n\rangle. \tag{4}$$

The normalization constant satisfies $N_l^{-2} = \exp(|\alpha|^2)\gamma(N+1, |\alpha|^2)/N!$. The lower limit on the Fock states implies that these states could be aptly termed as lower-truncated coherent states (LTCS). By construction, the UTCS and LTCS are orthogonal to each other. If $\alpha \to 0$, then $|\psi, N\rangle_u$ and $|\psi, N\rangle_l$ are $|0\rangle$ and $|N+1\rangle$ respectively. The canonical coherent state $|\alpha\rangle$ is expressed as

$$|\alpha\rangle = \frac{\exp(-|\alpha|^2/2)}{N_u N_l} \left[N_l |\alpha, N; u\rangle + N_u \alpha^{N+1} |\alpha, N; l\rangle\right]. \tag{5}$$

In this work, the properties of the LTCS are presented and compared with those of the UTCS. In Section II, the relation between the LTCS and another well known nonclassical state, namely, the photon-added coherent states (PACS) is established. Nonclassical features such as squeezing and sub-Poissonian statistics are discussed in Section III, followed by a summary of the results in Section IV.

2 LTCS and Photon-added coherent states

Photon-addition is mathematically represented by the action of a suitable creation operator on a state of the electromagnetic field. The process leads to generation of nonclassical states from the coherent states[7]. The process and its various generalizations have been studied both experimentally and theoretically[9]; see [22] for a recent review.

Photon-added coherent states (PACS) are defined as[7]

$$|\alpha, m\rangle \propto \hat{a}^{\dagger m}|\alpha\rangle = \exp(-\frac{|\alpha|^2}{2}) \sum_{n=0}^{\infty} \frac{\alpha^n \sqrt{(n+m)!}}{n!}|n+m\rangle. \qquad (6)$$

The parameter m is the order of the PACS. These states have been experimentally realized in optical parametric down-conversion[9]. Both the LTCS $|\alpha, N'l\rangle$ and the PACS $|\alpha, m\rangle$ with $m = (N+1)$ are defined are superpositions of the the same set of Fock states $\{|n\rangle\}$ $[n = m+1,\ m+2, \cdots]$. To see the connection between the two states, consider the deformed annihilation operator $\hat{A} = (1 + k\hat{a}^\dagger\hat{a})\hat{a}$, where k is nonnegative, not exceeding unity. Associated with $\hat{A}$ is the "deformed creation operator" $\hat{B}^\dagger = \hat{a}^\dagger(1 + k\hat{a}^\dagger\hat{a})^{-1}$,

and these two operators satisfy $\left[\hat{A}, \hat{B}^{\dagger}\right] = I$[23]. It is important to note that $\hat{B}^{\dagger}$ is not the adjoint of $\hat{A}$. Starting with the coherent state $|\alpha\rangle$, define

$$|\alpha, m\rangle_k = N_k \hat{B}^{\dagger m}|\alpha\rangle = N_k \sum_{n=0}^{\infty} \frac{\alpha^n}{n!} \frac{\sqrt{(n+m)!}}{\Pi_{j=0}^{m-1}(1+kn+kj)}|n+m\rangle. \qquad (7)$$

In the limit of vanishing k, the state $|\alpha, m\rangle_k$ becomes the m-PACS $|\alpha, m\rangle$; with $k = 1$, the state becomes the LTCS. Hence, the PACS and LTCS are the limiting cases of the deformed-PACS $|\alpha, m\rangle_k$. If $k = 1$, the creation operation $\hat{B}^{\dagger} = \hat{a}^{\dagger}(1+\hat{a}^{\dagger}\hat{a})^{-1}$ is the right inverse of the annihilation operator $\hat{a}$, that is, $\hat{a}\hat{B}^{\dagger} = I$[24]. Thus, the LTCS are the obtained by the repeated application of the right inverse of $\hat{a}$ on the coherent state $|\alpha\rangle$. The notion of deformed photon-addition has been discussed in the context of Posch-Teller potential[25] too. The overlap between the PACS and LTCS of same amplitude α and order $N+1$ is

$$|\langle \alpha, N+1|\alpha, N; l\rangle_l|^2 = \frac{|\alpha|^{2(N+1)}}{(N+1)\gamma(N+1, |\alpha|^2)L_{N+1}(-|\alpha|^2)}, \qquad (8)$$

where $L_N(x)$ is the Laguerre polynomial of order N[17]. For large values of N, the overlap becomes negligible indicating that the two limiting cases are nearly orthogonal to each other.

It is known that the PACS of order $N+1$ provide a resolution of identity for the subspace spanned by the number states $|N+1\rangle,\ |N+2\rangle,\ |N+3\rangle, \cdots$[26]. A similar relation holds for the LTCS too. In this case,

$$\frac{1}{\pi}\int d^2\alpha \frac{\gamma(N+1, |\alpha|^2)}{N!}|\alpha, N; l\rangle\langle\alpha, N; l| = I - \sum_{n=0}^{N}|n\rangle\langle n|. \qquad (9)$$

The RHS of the above equation is the identity operator on the subspace spanned by $|N+1\rangle, |N+2\rangle, |N+3\rangle, \cdots$. From the definition of the incomplete Gamma function given in Eq. 3, it is seen that $\gamma(N+1, x)$ is non-negative if $x \geq 0$. This means that the weight function in the resolution of identity by the LTCS is nonnegative.

The result that a LTCS of order $N+1$ is obtained by the action of the deformed creation operator $\hat{B}^{\dagger N}$ on the coherent state $|\alpha\rangle$ leads to a plausible method of generating these states, in close parallel to the suggestion by Agarwal and Tara[7] to generate the PACS. Consider a two-level atom interacting with a single-mode of the electromagnetic field. The Hamiltonian in the interaction picture is taken to be $H_I = \hbar\lambda\left[\hat{B}^{\dagger}\sigma_- + \hat{B}\sigma_+\right]$, which is a generalized Jaynes-Cummings model of atom-field interaction[27, 28]. This interaction corresponds to an intensity-dependent atom-field coupling. Here σ_+ and σ_- are respectively the raising and lowering operators for the atomic states $|e\rangle$ and $|g\rangle$ and λ is coupling constant. The actions of the raising and lowering operators on the atomic states are given by $\sigma_\pm|e\rangle = (|g\rangle \mp |g\rangle)/2$ and $\sigma_\pm|g\rangle = (|e\rangle \pm |e\rangle)/2$. The initial state of the atom-field state is $|\alpha\rangle|e\rangle$; the atom in the excited state $|e\rangle$ and the field in the coherent state $|\alpha\rangle$. If the interaction duration is small ($|t\lambda| << 1$), then the evolution operator is approximated to

$$\exp(-iH_I t/\hbar) \approx I - it\lambda\left[\hat{B}^{\dagger}\sigma_- + \hat{B}\sigma_+\right]. \tag{10}$$

The time-evolved state of the atom-field system is the superposition $|\alpha\rangle|e\rangle - it\lambda\hat{B}^{\dagger}|\alpha\rangle|g\rangle$, an entangled state of the system. Subsequent to the interaction,

if the atom is detected in its ground state $|g\rangle$, the field is in the state $\hat{B}^\dagger|\alpha\rangle$, which is the LTCS with $N = 0$. If another two-level atom in its excited state interacts with this resultant field $\hat{B}^\dagger|\alpha\rangle$, and the the atom is detected in its ground state after the interaction, the field changes to $\hat{B}^{\dagger 2}|\alpha\rangle$. After interacting with a sequence of N atoms which are subsequently detected in their respective ground states, the initial coherent state of the field is transformed to $\hat{B}^{\dagger N}|\alpha\rangle$, the LTCS of order N. It is possible to make the atom-field coupling to be time-dependent and its form can be tailored to generate arbitrary superpositions[30]. Another route to realize the type of the intensity-dependent coupling is to consider situations in which the rotating-wave approximation is not suitable and the resulting Hamiltonian is equivalent to including an intensity-dependent interaction of the form $(1 - k\hat{a}^\dagger\hat{a})\hat{a}$, which approximates the operator $(1 + k\hat{a}^\dagger\hat{a})^{-1}\hat{a}$ when $k\langle\hat{a}^\dagger\hat{a}\rangle < 1$[31], wherein the expectation value $\langle\hat{a}^\dagger\hat{a}\rangle$ is in the state $|\alpha, N; l\rangle$. Further, it has been shown that the properties of a cavity containing nonlinear media can be tuned to provide different forms of intensity-dependent atom-field couplings[32].

Another state that is relevant in the context of the commutation $\left[\hat{A}, \hat{B}^\dagger\right] = I$ is $\exp(\alpha\hat{B}^\dagger - \alpha^*\hat{A})|0\rangle$, whose Fock basis expansion is

$$\exp(\alpha\hat{B}^\dagger - \alpha\hat{A})|0\rangle \propto \sum_{n=0}^{\infty} \frac{\alpha^n}{\sqrt{n!}} \frac{1}{(1+k)(1+2k)\cdots(1+(n-1)k)}|n\rangle. \quad (11)$$

Since $\hat{B}^\dagger$ is not the adjoint of A, the operator $\exp(\alpha\hat{B}^\dagger - \alpha^*\hat{A})$ is not unitary. However, its action on the vacuum results in a state that is normalizable for all values of α. In this work, these states are not discussed further.

3 Nonclassical features

Pure states of the electromagnetic field, except the coherent states, are nonclassical. Squeezing and sub-Poissonian statistics are two of the experimentally verifiable nonclassical features that a state of the electromagnetic field can exhibit. In this section, these two aspects of the LTCS are discussed. If the deforming parameter $k = 1$, the expectation of the annihilation operator and creations operators are

$$\langle \hat{a} \rangle_u = \langle \hat{a}^\dagger \rangle_u^* = N\alpha \frac{(N-1)! - \gamma(N-1, |\alpha|^2)}{N! - \gamma(N, |\alpha|^2)} \tag{12}$$

$$\langle \hat{a}^2 \rangle_u = \langle \hat{a}^{\dagger 2} \rangle_u^* = N(N-1)\alpha^2 \frac{(N-1)! - \gamma(N-1, |\alpha|^2)}{N! - \gamma(N, |\alpha|^2)}, \tag{13}$$

$$\langle \hat{a} \rangle_l = \langle \hat{a}^\dagger \rangle_l^* = \alpha, \tag{14}$$

$$\langle \hat{a}^2 \rangle_l = \langle \hat{a}^{\dagger 2} \rangle_l^* = \alpha^2. \tag{15}$$

The subscripts u and l refer to the UTCS and LTCS respectively. An interesting feature is that the expectations values of the two operators in LTCS are independent of N. However, the expectation value of the number operator $\hat{a}^\dagger \hat{a}$ does not possess this feature,

$$\langle \hat{a}^\dagger \hat{a} \rangle_u = N \frac{(N-1)! - \gamma(N-1, |\alpha|^2)}{N! - \gamma(N, |\alpha|^2)} |\alpha|^2 \tag{16}$$

$$\langle \hat{a}^\dagger \hat{a} \rangle_l = N|\alpha|^2 \frac{\gamma(N, |\alpha|^2)}{\gamma(N+1, |\alpha|^2)} \tag{17}$$

3.1 Squeezing in X and P quadratures

For the single mode electromagnetic field, the following quadratures are defined,

$$\hat{X} = \frac{\hat{a}^\dagger + \hat{a}}{\sqrt{2}} \qquad \hat{P} = \frac{\hat{a} - \hat{a}^\dagger}{i\sqrt{2}}. \tag{18}$$

The corresponding uncertainties are $(\Delta X)^2 = \langle \hat{X}^2 \rangle - \langle \hat{X} \rangle^2$ and $(\Delta P)^2 = \langle \hat{P}^2 \rangle - \langle \hat{P} \rangle^2$. For the coherent states of the electromagnetic field, uncertainties in the two quadratures are equal to 1/2. A state is said to exhibit squeezing in a quadrature if the uncertainty in that quadrature is smaller than 1/2. The PACS, which corresponds to $k = 0$ in $|\alpha, m\rangle_k$, exhibits squeezing. In Fig. 1, the uncertainty in X quadrature is shown as a function of the parameter k, for three different values of N. The lowest values of ΔX are achieved for the PACS ($k = 0$ case in the figure). However, squeezing occurs over a substantial range of k. If $N < |\alpha|^2$, the amount of squeezing in the X-quadrature is larger for smaller N. The range of k over which squeezing occurs, however, decreases as N increases.

In this work, the focus is on the properties of the LTCS. Explicit expressions for the uncertainties in the LTCS are

$$(\Delta X)_l^2 = (\Delta P)_l^2 = \frac{1}{2}\left[1 + 2|\alpha|^2\left[(N+1)\frac{\gamma(N, |\alpha|^2)}{\gamma(N+1, |\alpha|^2)} - 1\right]\right]. \tag{19}$$

In Fig. 2 , the variation of ΔX and ΔP are shown for different values of N for the LTCS corresponding to $\alpha = \sqrt{10}$.

It is seen from the figures that the quantities ΔX and ΔP are nearly equal to those of the coherent state α, for $N \leq |\alpha|^2$, though the average

number of photons is high. If the condition on N is satisfied, the states $|\psi\rangle_l$ are MUS with equal variances in the quadratures, whereas the squeezed vacuum is a MUS though with unequal distribution of fluctuations. Unlike in the case of the PACS, the uncertainties in the two quadratures are equal for the LTCS, which holds for the number states and coherent states too. This, in turn, means that LTCS cannot exhibit reduced fluctuation in any of the quadratures, whereas PACS exhibits squeezing.

For comparison, uncertainty profiles for the UTCS are also given in Fig. 2. In the state $|\psi, N\rangle_u$, squeezing occurs if the magnitude of α is small. In that limit, UTCS is well approximated by a superposition of the vacuum state $|0\rangle$ and the single photon state $|1\rangle$. Such states are known as Bernoulli states and they exhibit squeezing[29].

The overlap $|\langle\alpha|\alpha, N\rangle_l|^2$ between the coherent state $|\alpha\rangle$ and the UTCS is $\exp(-|\alpha|^2)\sum_{n=0}^{N}|\alpha|^{2n}/n!$. If $N >> |\alpha|^2$, the summation is nearly $\exp(|\alpha|^2)$ and the overlap is almost equal to unity. In that case, the UTCS is almost the coherent state $|\alpha\rangle$, which is a MUS. It is interesting to note that for the UTCS the maximum uncertainties in the quadratures occur when $N \approx |\alpha|^2/\sqrt{2}$.

3.2 Phase distribution

Phase distribution of a quantum state of the electromagnetic field provides information about uncertainty in the phase of the field. This, in turn, imposes a lower limit on the the fluctuations in the number of photons. An useful approach to define phase distribution is the Pegg-Barnett formulation

[33]. Phase distribution of an arbitrary state of the field is obtained by the overlap of the state with the phase state

$$|\theta\rangle = \frac{1}{\sqrt{1+s}} \sum_{n=0}^{s} e^{in\theta}|n\rangle. \tag{20}$$

and taking the limit $s \to \infty$. The respective phase distributions for the states $|\psi\rangle_u$ and $|\psi\rangle_l$ are

$$P_u(\theta) = \lim_{s\to\infty} \frac{s+1}{2\pi}|\langle\theta|\psi\rangle_u|^2 = N_u^2 \left| \sum_{n=0}^{N} \frac{\exp(-in\theta)\alpha^n}{\sqrt{n!}} \right|^2, \tag{21}$$

and

$$P_l(\theta) = \lim_{s\to\infty} \frac{s+1}{2\pi}|\langle\theta|\psi\rangle_l|^2 = N_l^2 \left| \sum_{n=N+1}^{\infty} \frac{\exp(-in\theta)\alpha^n}{\sqrt{n!}} \right|^2. \tag{22}$$

The phase distributions for the UTCS and LTCS are shown in Figs. 3 and 4 respectively, for three different values of N. As the cutoff N increases, the phase-distribution of UTCS approaches that of a coherent state of amplitude α. In the case of LTCS, the phase-distribution broadens as N increases. This feature is shown in Fig. 4. If $N >> |\alpha|^2$, the LTCS is a superposition of the states $|N+1\rangle$ and $|N+2\rangle$,

$$|\alpha, N; l\rangle \approx \sqrt{\frac{N+2}{2+N+|\alpha|^2}} \left[|N+1\rangle + \frac{\alpha}{\sqrt{N+2}}|N+2\rangle \right]. \tag{23}$$

Such a superposition has a fairly well defined number of quanta, the corresponding uncertainty in the number of photons is

$$(\Delta n)^2 = \langle \hat{a}^\dagger \hat{a} \hat{a}^\dagger \hat{a} \rangle - \langle \hat{a}^\dagger \hat{a} \rangle^2 = \frac{|\alpha|^2(2+N)}{(2+|\alpha|^2+N)^2}. \tag{24}$$

If $N >> |\alpha|^2$, then $\Delta n << 1$, that is, the photon number fluctuation is small. Consequently, the phase distribution is broad.

The photon-number distribution of the LTCS is not Poissonian. Whether it is sub-Poissonian or not is inferred from the Q-parameter introduced by Mandel[34],

$$Q = \frac{\langle \Delta n \rangle^2}{\langle \hat{a}^\dagger \hat{a} \rangle} - 1 = \frac{|\alpha|^2}{(2 + N + |\alpha|^2)(1 + N + |\alpha|^2)} - 1 < 0. \qquad (25)$$

for the state given in Eq. 23, which is the large-N limit of the LTCS. This parameter is used to quantify the deviation from the Poissonian distribution. Consequently, the Q-parameter assumes negative values signalling the sub-Poissonian nature of the LTCS. Though the above closed form expressions have been obtained taking N to be large, numerical evaluation of Q for the exact LTCS shows that the states are indeed sub-Poissonian. The N-dependence of the Q parameter is shown in Fig. 5. It is seen that for all values of N the Q-parameter is negative.

3.3 Entanglement Potential

Nonclassicality of a quantum state is amenable to quantification and many measures of nonclassicality are known: nonclassical distance[35, 36], nonclassical depth[37], phase-space volume of the negative regions of the Wigner distribution[38], etc. Of these, the criterion based on the Wigner function is measurable as the Wigner function of a quantum state can be constructed by measuring a suitably chosen set of observables[39, 40, 41]. Recently, Asboth *et al* proposed a measure of nonclassicality of any quantum state of

a single-mode of the electromagnetic field[42]. Beam-splitter is a device in which two input modes interact to generate two output modes. In principle, due to the interaction, the output modes can be entangled. A necessary condition for a beam-splitter to generate entangled output state is that at least one of the inputs should be a nonclassical[43, 44]. This feature has been used to define a new measure of nonclasciality called entanglement potential. It is the amount of entanglement between the two output modes when the input ports are fed with states $|0\rangle|\psi\rangle$, where $|0\rangle$ is the vacuum of one of the modes and the $|\psi\rangle$ is the state of field input in the other mode. Though both the LTCS and UTCS are nonclassical states, it is important to compare the entanglement potentials of the two states. Each of the input ports of a beam-splitter is modelled as a mode. The unitary operator representing the action of a beam-splitter is $\exp[\Gamma\hat{a}^\dagger\hat{b} - \Gamma^*\hat{a}\hat{b}^\dagger]$, Γ represents the complex transmittance of the beam splitter[28]. Here $\hat{a}$ and $\hat{a}^\dagger$ are the annihilation and creation operators for one of the input ports. For the other input port, the corresponding operators are $\hat{b}$ and $\hat{b}^\dagger$. The operators $K_+ = \hat{a}^\dagger\hat{b}$, $K_- = \hat{a}\hat{b}^\dagger$ and $K_0 = (\hat{a}^\dagger\hat{a} - \hat{b}^\dagger\hat{b})/2$ are generators of the SU(1,1) algebra. One form of disentangled representation of the unitary operator is

$$\exp(\Gamma K_+ - \Gamma^* K_+) = \exp(2\ln|\Gamma| K_+)\exp(-e^{-i\theta}\tan|\Gamma| K_0)\exp(e^{i\theta}\tan|\Gamma| K_-), \tag{26}$$

where $\Gamma = |\Gamma|\exp(i\theta)$[45]. If vacuum is the input in one of the input ports and $|\psi\rangle = \sum_{n=0}^{\infty} c_n|n\rangle$ in the other input port, the output state $|\chi\rangle$ is

$$|\chi\rangle = \sum_{n=0}^{\infty} c_n \exp(nB) \sum_{k=0}^{n} A^k \sqrt{{}^nC_k}|n-k\rangle|k\rangle. \tag{27}$$

Then the reduced density operator for the a-mode is

$$\rho_a = \sum_{n,m=0}^{\infty} c_n c_m^* \exp(B(n+m)) \sum_{k=0}^{\min(n,m)} \frac{|A|^{2k}}{k!} \sqrt{{}^nC_k} \sqrt{{}^mC_k} |n-k\rangle\langle m-k|, \tag{28}$$

where $B = -e^{-i\theta} \tan|\Gamma|$ and $A = 2 \log \sec|\Gamma|$. For 50-50, symmetric beam splitter, $\Gamma = i\pi/4$. The coefficients c_n are those of the LTCS or UTCS depending on which state of the field is used in the input port of the beam-splitter.

A measure of entanglement for two-mode, pure states is the mixedness of the reduced density operator of one of the subsystems, and linear entropy $1 - Tr[\tilde{\rho}_a^2]$, quantifies the mixedness[46]. Hence, the entanglement between the output field modes is measured by the linear entropy of one of the output modes. The amount of entanglement introduced by the beam-splitter is a measure of nonclassicality of the input field[42]. In Fig. 6, the linear entropy of the reduced density operator for the output from the beam-splitter is shown. With the UTCS and vacuum as the input fields, the linear entropy decreases as the number of Fock states in the UTCS increases. Higher the cutoff, the UTCS approximates the coherent state $|\alpha\rangle$; consequently, the output fields are less entangled. The entanglement potential of the LTCS increases as the cutoff N increases, a feature shared by the PACS as well[47]. As N increases, the LTCS is essentially the number state $|N\rangle$, as evident from the large N limit of Eq. 23 and the entanglement potential of the number state increases with N. Since the nonclassicality of the UTCS decreases with N and that of the LTCS increases, there exists a value of the cutoff parameter at which the states have nearly the same entanglement

potential. If amplitude $\alpha = \sqrt{10}$, the entanglement potential of the two states are nearly equal if the cut-off parameter $N = 4$.

Recently, the entanglement potential of the PACS has been studied in detail[48]. Since the LTCS and PACS of equal order are defined on the same sector of the Hilbert space, it is of interest to compare the entanglement potential of these states. The expression for the reduced density operator given in Eq. 28 is used with the coefficients c_n being those of the PACS given in Eq. 6. In Fig. 7, the entanglement potential of the LTCS of order N is compared with the PACS of same order for $N = 1$ 2,3 and 4. It is seen that the LTCS has higher entanglement potential compared to the PACS. This, in turn, means that the LTCS are better suited for generating entangled output modes in a beam-splitter than the PACS. Currently, a comparison of the two states in the context of quantum teleportation is being investigated, the results of which will be presented elsewhere.

4 Summary

The states obtained by removing a set of contiguous, low energy Fock states from the coherent states of the electromagnetic field are non-Gaussian and nonclassical. These truncated coherent states possess equal uncertainties in the two quadratures, and do not exhibit squeezing. Additionally, if the cutoff parameter N is less than $|\alpha|^2$, the product of the uncertainties attains its minimum, like that of the coherent states. In this approximation, these states are minimum uncertainty states whose average photon number is large (because $|\alpha|$ is large), but the photon statistics is sub-Poissonian.

These states provide a resolution of identity for the subspace spanned by the Fock states $|N+1\rangle,\ |N+2\rangle,\ |N+3\rangle, \cdots$. The noncalssicality, quantified by the entanglement potential, of the truncated states increases as the cutoff N increases. This is related to the fact that if $N > |\alpha|^2$, the states are well approximated by a superposition the successive Fock states $|N+1\rangle$ and $|N+2\rangle$, which is the generalized Bernoulli state. Further, the entanglement potential of the truncated coherent states is higher than that of the photon-added coherent states of same amplitude and order. The photon-added coherent states and the lower truncated coherent states are the limiting cases of a suitably deformed photon-added coherent state, wherein the deformation is effected by a function of the number operator. The photon-added coherent states exhibit squeezing which is absent in truncated coherent states. The states which interpolate between these two liming cases show squeezing. Further, the entanglement potential of truncated coherent states is always higher than that of the photon-added coherent states. The Jaynes-Cummings hamilotnian without rotating wave approximation is the type of interaction required to produce these interpolating states.

References

[1] R. J. Glauber, Coherent and incoherent states of the radiation field, Phys. Rev. **131**, 2766-2788(1963).

[2] E. C. G. Sudarshan, Equivalence of Semiclassical and Quantum Mechanical Descriptions of Statistical Light Beams, Phys. Rev. Lett. **10**, 277-279(1963).

[3] C. C. Gerry and P. L. Knight, Introductory Quantum Optics, Cambridge University Press, New York (2005).

[4] B. Yurke and D. Stoler, Generating quantum mechanical superpositions of macroscopically distinguishable states via amplitude dispersion, Phys. Rev. Lett. **57**, 13-16(1986).

[5] V. Buzek, A. Vidiella-Barranco and P. L. Knight, Superpositions of coherent states: Squeezing and dissipation, Phys. Rev. A **45**, 6570-6585(1992).

[6] A. Ourjoumtsev, H. Jeong, R. Tualle-Brouri and P. Grangier, Generation of optical 'Schrodinger cats' from photon number states, Nature **448** 784-786 (2007).

[7] G. S. Agarwal and K. Tara, Nonclassical properties of states generated by the excitations on a coherent state, Phys. Rev. A **43**, 492-497(1991).

[8] J. Lee, J. Kim and H. Nha, Demonstrating higher-order nonclassical effects by photon-added classical states: realistic schemes, J. Opt. Soc. Am. B **26**, 1363-1369(2009).

[9] A. Zavatta, S. Viciani and M. Bellini,Quantum-to-Classical Transition with Single-Photon-Added Coherent States of Light , Science **306**, 660-662(2004).

[10] S. A. Babichev, J. Ries and A. I. Lvovsky, Quantum scissors: Teleportation of single-mode optical states by means of a nonlocal single photon, Europhys. Lett **64**, 1-7(2003).

[11] F. Ferreyrol, M. Barbieri, R. Blandino, S. Fossier, R. Tualle-Brouri and P. Grangier, Implementation of a Nondeterministic Optical Noiseless Amplifier, Phys. Rev. Lett. **104**, 123603(2010).

[12] P. Marek, H. Jeong and M. S. Kim, Generating "squeezed" superpositions of coherent states using photon addition and subtraction, Phys. Rev. A **78**, 063811 (2008).

[13] L. M. Kuang, F. B. Wang and Y. G. Zhou, Coherent States of a Harmonic Oscillator in a Finite-dimensional Hilbert Space and Their Squeezing Properties, J. Mod. Opt. **41**, 1307-1318(1994).

[14] W. Leonski and Kowalewska-Kudlaszyc, Quantum Scissors-Finite dimensional States Engineering, Progress in Optics **56**, 131-185(2011).

[15] A. Miranowics, K. Piatek and R. Tanas, Coherent states in a finite-dimensional Hilbert space, Phys. Rev. A **50** 3423-3426 (1994).

[16] W. Leonski, Finite-dimensional coherent-state generation and quantum-optical oscillator models, Phys. Rev. A **55** 3874-3878 (1997).

[17] I. S. Gradshteyn and I. M. Ryzhik, Table of Integral, Series and Products, Academic Press, USA, 2000.

[18] D. T. Pegg, L. S. Philips and S. M. Barnett, Optical State Truncation by Projection Synthesis, Phys. Rev. Lett. **81**, 1604-1606(1998).

[19] L. M. Kuang, F. B. Wang and Y. G. Zhou, Dynamics of a harmonic oscillator in a finite-dimensional Hilbert space, Phys. Lett. A **183**, 1-8(1993).

[20] A. Miranowicz, W. Leonski and N. Imoto, Quantum-Optical States in Finite-Dimensional Hilbert Space. I. General Formalism, Advances in Chemical Physics, **119**, 155-194 (2001).

[21] W. Leonski and A. Miranowicz, Quantum-Optical States in Finite-Dimensional Hilbert Space. II. State Generation, Advances in Chemical Physics, **119**, 194-214 (2001).

[22] M. S. Kim, Recent developments in photon-level operations on travelling light fields, J. Phys. B: At. Mol. Opt. Phys. **41**, 133001(2008).

[23] P. Shanta, S. Chaturvedi. V. Srinivasan, G. S. Agarwal and C. L. Mehta, Unified approach to multiphoton coherent states, Phys. Rev. Lett. **72**, 1447-1450(1994).

[24] A. K. Roy and C. L Mehta, Boson inverse operators and associated coherent states, J. OPt. B:Quantum Semiclass. Opt. **7**, 877-888(1995).

[25] O. Safaeian and M. K. Tavassoly, Deformed photon-added nonlinear coherent states and their non-classical properties, J. Phys. A: Math. Theor. **44**, 225301(2011).

[26] J-M. Sixdeniers and K. A. Penson, On the completeness of photon-added coherent states, J. Phys. A: Math. and Gen. **34**, 2859-2866(2001).

[27] B. Buck and C. V. Sukumar, Exactly soluble model of atom-phonon coupling showing periodic decay and revival, Phys. Lett. A **81**, 132-135 (1981).

[28] W. Vogel, D. G. Welsch and S. Wallentowitz, Quantum Optics An Introduction, Wiley-VCH, Berlin (2001).

[29] D. Stoler, B. E. A. Saleh and M. C. Teich, Binomial States of the Quantized Radiation Field, Optica Acts **32**, 345-355(1985).

[30] C. K. Law and J. H. Eberly, Arbitrary control of a quantum electromagnetic field, Phys Rev. Lett. **76**, 1055-1058(1996).

[31] M. H. Naderi, The Jaynes-Cummings model beyond the rotating-wave approximation as an intensity-dependent model: quantum statistical and phase properties, J. Phys. A: Math. Thoer. **44**, 055304 (2011).

[32] T. Hayrynen, J. Oksanen and J. Tulkki, Nonlinear laser cavities as nonclassical light sources, Eur. Phys. Lett. **100**, 54001 (2013).

[33] D. T. Pegg and S. M. Barnett, Phase properties of the quantized single-mode electromagnetic field, Phys. Rev. A **39** 1665-1675 (1989).

[34] L. Mandel, Sub-Poissonian photon statistics in resonance fluorescence, Opt. Lett. **4**, 205-207(1979).

[35] M. Hillery, Nonclassical distance in quantum optics, Phys. Rev. A **35**, 725-732(1987).

[36] A. Wunsche, V. V. Dodonov, O. V. Man'ko and V. I. Man'ko, Nonclassicality of States in Quantum Optics, Fortschr. Phys. **49**, 1117-1122(2001).

[37] C. T. Lee, Measure of the nonclassicality of nonclassical states, Phys. Rev. A **44**, R2775-R2778(1991).

[38] A. Kenfack and K. Zyczkowski, Negativity of the Wigner function as an indicator of non-classicality, J. Opt. B: Quan. and Semiclss. Opt **6**, 396-404(2004).

[39] W. Vogel and H. Risken, Determination of quasiprobability distributions in terms of probability distributions for the rotated quadrature phase, Phys. Rev. A **40**, 2847-2849(1989).

[40] D. T. Smithey, M. Beck, M. G. Raymer and A. Faridani, Measurement of the Wigner distribution and the density matrix of a light mode using optical homodyne tomography: Application to squeezed states and the vacuum, Phys. Rev. Lett. **70**, 1244-1247(1993).

[41] U. Leonhardt, *Measuring the Quantum State of Light* (Oxford University Press, Oxford, England, 1997).

[42] J. K. Asboth, J. Calsamiglia and H. Ritsch, Computable Measure of Nonclassicality for Light, Phys. Rev. Lett. **94**, 173602(2005).

[43] M. S. Kim, W. Son, V. Buzek, P. L. Knight, Entanglement by a beam splitter: Nonclassicality as a prerequisite for entanglement, Phys. Rev. A **65**, 032323(2002).

[44] Wang Xiang-bin, Theorem for the beam-splitter entangler, Phys. Rev. A **66**, 024303(2002).

[45] Ananda DasGupta, Disentanglement formulas: An alternative derivation and some applications to squeezed coherent states, Am. J. Phys. **64**, 1422-1427(1996).

[46] C. H. Bennett, H. J. Bernstein, S. Popescu and B. Schumacher, Concentrating partial entanglement by local operations, Phys. Rev. A **53** 2046-2052(1996).

[47] A. R. Usha Devi, R. Prabhu and M. S. Uma, Non-classicality of photon added coherent and thermal radiations, Eur. Phys. J. D **40**, 133-138(2006).

[48] K. Berrada, S. Abdel-Khalek, H. Eleuch and Y. Hassouni, Beam splitting and entanglement generation: excited coherent states, Quant. Inf. Proc. **12**, 69-82 (2013).

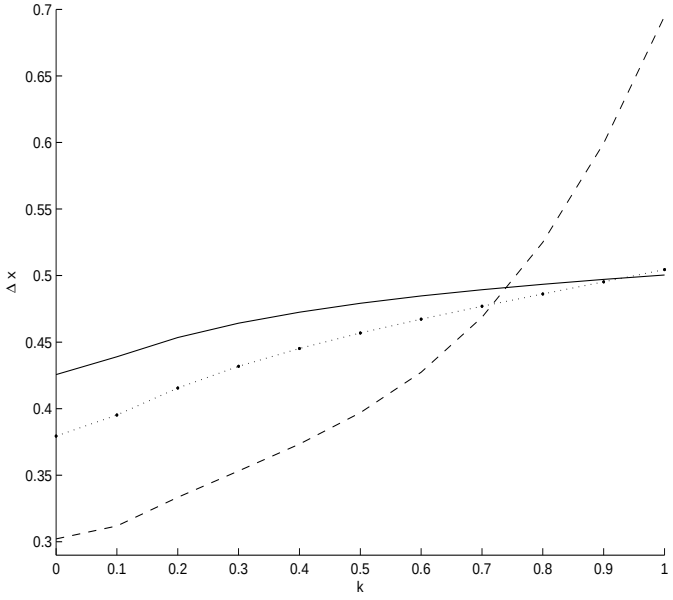

Figure 1: Uncertainty in X-quadrature as a function of the parameter k for states $|\alpha, N\rangle_k$, with $N = 2$ (continuous), $N = 3$ (line with dots) and $N = 5$ (dashed). In all cases $\alpha = \sqrt{10}$. The limiting cases corresponding to $k = 0$ and 1 are the PACS and LTCS respectively.

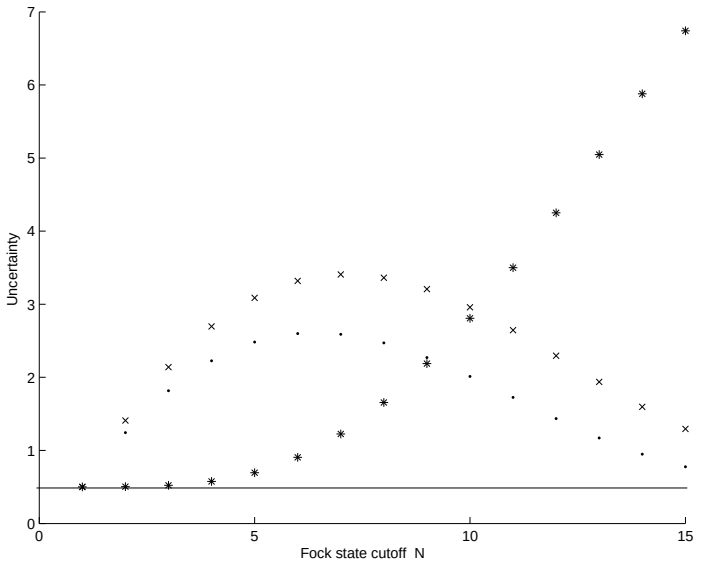

Figure 2: Uncertainty profiles of $X-$ and $P-$quadratures for the UTCS and LTCS as a function of the cutoff number N. For the UTCS, ΔX ($\times$) and ΔP (.)are shown; for LTCS ΔX(*) is shown, which is also the profile for ΔP. In all cases $\alpha = \sqrt{10}$.

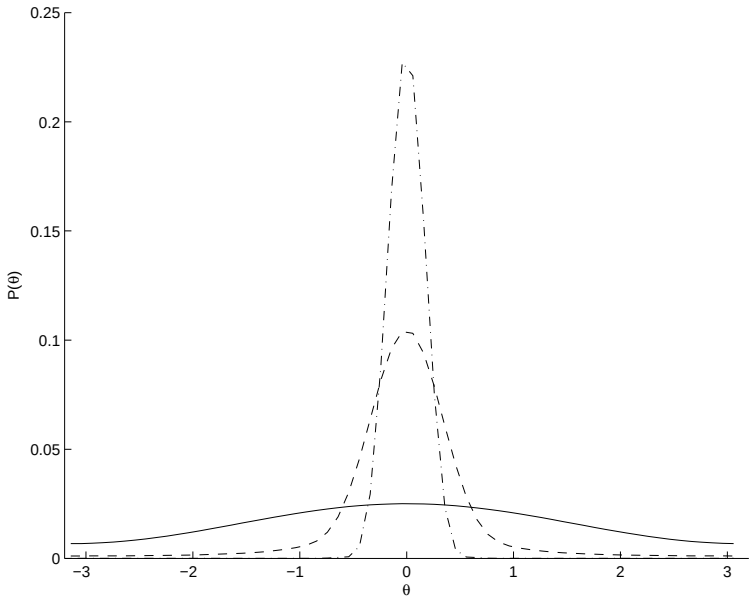

Figure 3: Phase distribution $P_u(\theta)$ for the UTCS for two different values of the cutoff parameter, $N = 2$ (continuous), $N = 10$ (dashed) and $N = 20$ (dot-dash). The amplitude $\alpha = \sqrt{10}$.

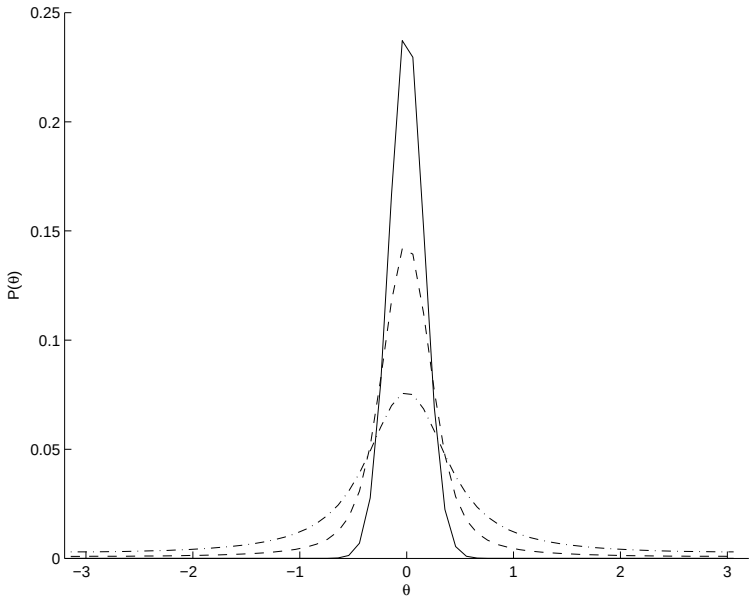

Figure 4: Phase distribution $P_l(\theta)$ for the LTCS for two different values of the cutoff parameter, $N = 2$ (continuous), $N = 10$ (dashed) and $N = 20$(dot-dash). The amplitude $\alpha = \sqrt{10}$.

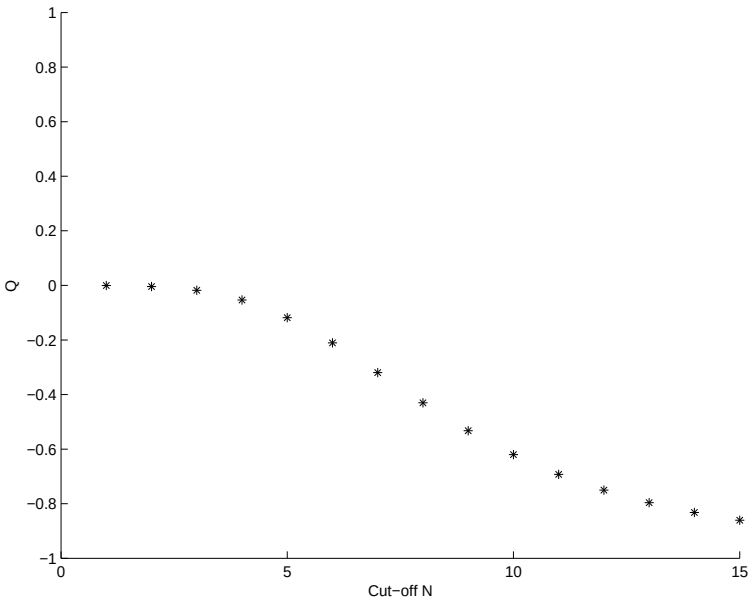

Figure 5: Q-parameter as a function of the cut-off parameter N for the LTCS of amplitude $\alpha = \sqrt{10}$.

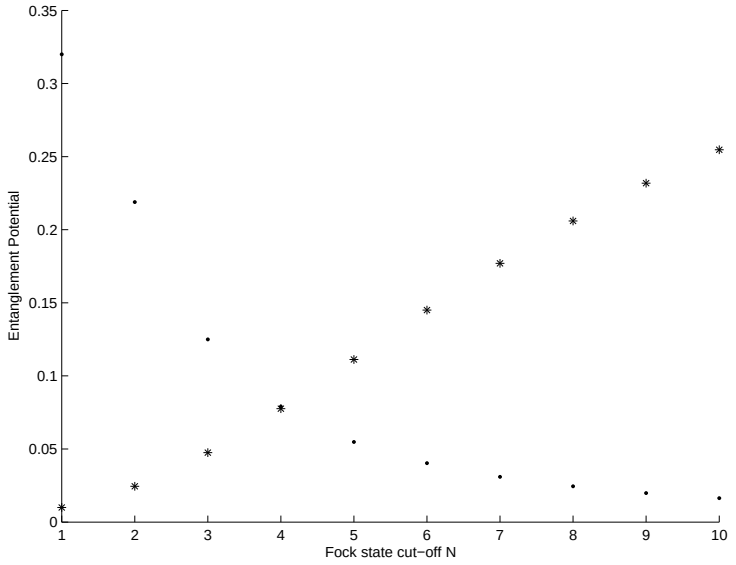

Figure 6: Entanglement potential as a function of the cut-off N for the UTCS (dots) and LTCS (star) of amplitude $\alpha = \sqrt{10}$.

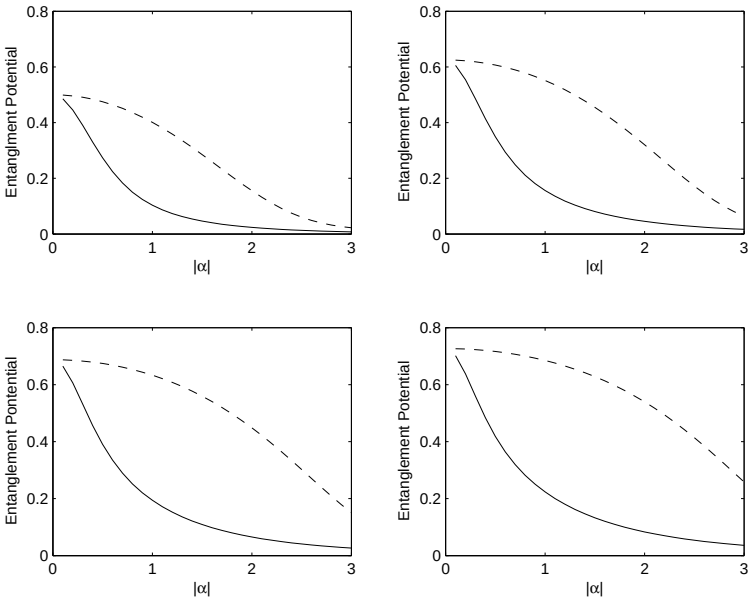

Figure 7: Entanglement potential as a function of $|\alpha|$ for the PACS(continuous) and LTCS (dash). Figs. (a)-(d) correspond to the lower cutoff values N=1,2,3 and 4 respectively.